

Mass-metallicity relation and fundamental metallicity relation at $z \gtrsim 2$

F. Cullen¹, M. Cirasuolo^{1,2}, R.J. McLure¹, J.S. Dunlop¹, and R.A.A. Bowler¹

¹ SUPA, Institute for Astronomy, University of Edinburgh, Royal Observatory, Edinburgh EH9 3HJ, e-mail: fc@roe.ac.uk

² UK Astronomy Technology Centre, Science and Technology Facilities Council, Royal Observatory, Edinburgh, EH9 3HJ

Abstract. We present results from the 3D-HST near-IR grism spectroscopic survey investigating the stellar mass, gas-phase metallicity (hereafter metallicity) and star-formation rate of a sample of star-forming galaxies at $z \gtrsim 2$. We determine the mass-metallicity relation for our sample and explore our results in the context of the fundamental metallicity relation. We find a mass-metallicity relation consistent with previous determinations out to $z \sim 3 - 4$ in that we observe a decrease in metallicity with decrease in stellar mass. However, in contrast to previous results, we find our $z \gtrsim 2$ sample is not consistent with the FMR defined in the local Universe. We explore this discrepancy in terms of recent theoretical determinations of the evolution of star-forming galaxies in the BPT diagram. We show that, for metallicity calibrations derived using local Universe galaxies, this evolution may affect metallicities determined from different sets of nebular emission line ratios. We discuss the implications of this differential evolution of metallicity line diagnostics on the current interpretation of the FMR and its evolution at $z \gtrsim 2.5$. Our results caution against the use of local empirical metallicity calibrations in high redshift galaxies.

Key words. galaxies: high redshift – galaxies: metallicities – galaxies: nebular emission lines – galaxies: ionization conditions

1. Introduction

The mass-metallicity relation (MZR) has now been established across the past ~ 11 Gyr of cosmic time, from the local Universe (e.g. Tremonti et al. 2004) out to $z \sim 3$ (e.g. Maiolino et al. 2008). A consistent picture has begun to emerge from these various studies of a relation similar in shape but differing in normalization out to high redshift: at a given redshift, galaxies with lower stellar mass are found to have lower metallicities, and at

a given mass, galaxies at higher redshift are found to have lower metallicities.

Incorporating star-formation rate information into the MZR, Mannucci et al. (2010) formulated the so-called “fundamental metallicity relation” (FMR), which linked the redshift evolution of the MZR with the increase in SFR of the star-forming galaxy population between $0 < z < 2$. The FMR states that at a given stellar mass, a galaxy with higher SFR will have a lower gas phase metallicity due to the large reservoir of pristine gas triggering the observed burst of star formation. In this context, the evo-

lution to lower metallicities with redshift is explained by the observed increase in the SFR of galaxies with redshift (e.g. Daddi et al. 2007).

In their original paper Mannucci et al. (2010) found that local star-forming galaxies lie on the 3-dimensional surface defined by the FMR with a low residual dispersion (0.05 dex), and that galaxies out to $z \sim 2.5$ are consistent with the FMR defined locally. However they observed an apparent evolution of galaxies away from the FMR at $z > 2.5$ indicative of some change in the physical process regulating the evolution of galaxies at these redshifts. More data is needed at this crucial epoch ($2 < z < 3$) to explore the evolution of the FMR further.

2. 3D-HST survey

The spectroscopic data that make up our sample are drawn from the 3D-HST grism spectroscopic survey (Brammer et al. 2012). Within the redshift range $2.0 < z < 2.3$ the grism spectra allow us to measure the fluxes of the $[\text{OIII}]\lambda 4958, 5007$, $\text{H}\beta$ and $[\text{OII}]\lambda 3727$ nebular emission lines and the ratios of these lines allow the determination of the gas-phase metallicity (Maiolino et al. 2008). SFRs can be measured from the $\text{H}\beta$ line flux corrected for dust extinction and the stellar masses from ancillary photometric data (from the rest-frame UV to mid-infrared) taken as part of the CANDELS survey (Grogin et al. 2011; Koekemoer et al. 2011). The sample was selected from an independent reduction of the 3D-HST grism data across the GOODS-S, COSMOS and UDS fields. Galaxies were visually inspected to ensure secure redshifts and AGN were rejected from the sample using X-ray data where available or a modified version of the MEx AGN selection technique (Juneau et al. 2011). The final sample consists of 93 galaxies. Because of the low signal to noise of the individual grism spectra the galaxies were stacked into 6 bins of stellar mass. This follows directly the method adopted for the previous determination of the MZR at $z \geq 2$ of Erb et al. (2006). A detailed description of sample selection and reduction is given in Cullen et al. (2013)

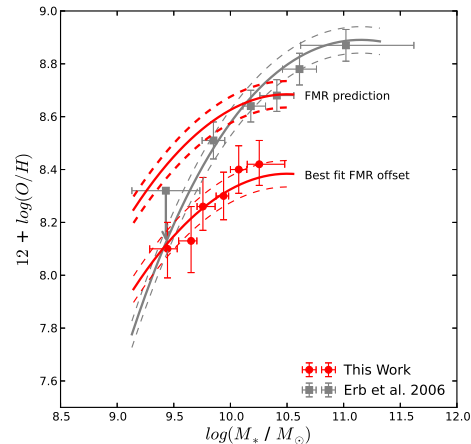


Fig. 1. Mass-metallicity relation observed at $z \geq 2$ for our sample (red circles) and the sample of Erb et al. (2006) (grey squares) compared to the predictions from the FMR (solid lines). For our data we show the both the FMR prediction for the position of the galaxies in the MZR plane, and the best fitting FMR offset to our data. For the Erb et al. (2006) data we show only the FMR prediction since their data is consistent with the FMR.

3. MZR and FMR at $z \geq 2$

Fig. 1 shows the inferred mass-metallicity relation for our sample at $z \geq 2$ compared to the previous sample of Erb et al. (2006). The MZR of our sample is consistent with previous determinations of the MZR from the local Universe out to $z \sim 3$ in that the metallicity of our galaxy stacks increases with increasing stellar mass. We observe a metallicity increase of ~ 0.3 dex over a ~ 0.8 dex range in stellar mass. However, at a given stellar mass our galaxies are offset to lower metallicities by ~ 0.3 dex compared to the Erb et al. (2006) data.

The offset in metallicities can be interpreted in terms of the SFR of the stacks. According to the FMR if the SFRs of our mass bins are higher than the SFRs of the Erb et al. (2006) mass bins we would expect an offset to lower metallicities. However, the SFR of our sample are in fact on average lower across the full range of stellar masses (see Cullen et al.

2013). This implies one or both of the datasets are inconsistent with the FMR.

Mannucci et al. (2010) showed that the Erb et al. (2006) data are consistent with the FMR and we reproduce this result in Fig. 2, in which the difference between measured metallicity and metallicity predicted from the FMR is compared for different datasets. Our data are inconsistent with the FMR. As illustrated in Fig. 3, the metallicities of our mass bins are offset by an average of -0.3 dex from the FMR prediction.

This FMR offset is comparable to the ~ -0.5 dex offset of the $z \sim 3 - 4$ galaxies from the AMAZE/LSD surveys (Maiolino et al. 2008; Mannucci et al. 2009). A critical similarity between our data and the AMAZE/LSD data is the line diagnostics used for deriving metallicities (oxygen and $H\beta$ lines). The Erb et al. (2006) metallicities are by contrast derived from the $[\text{NII}]/\text{H}\alpha$ ratio. Though all line ratios are calibrated to the same metallicity scale (Maiolino et al. 2008), these calibrations were made empirically using local galaxy spectra, and since the line ratios are not purely metallicity dependent, using local calibrations at high redshift assumes the physical conditions of star-forming regions do not evolve strongly (see Kewley & Ellison 2008 for a detailed discussion of different types of metallicity calibration). Any differential evolution of the line ratios which is not metallicity dependent may cause a discrepancy in derived metallicities at high redshifts using empirical calibrations.

4. Photoionization conditions

Fig. 3 shows the BPT diagram (Baldwin, Phillips & Terlevich 1981). The BPT diagram is a plot of $[\text{OIII}]\lambda 5007/\text{H}\beta$ vs $[\text{NII}]/\text{H}\alpha$ and is used for diagnosing ionization conditions in star-forming galaxies and AGN. Current observations suggest that galaxies at high redshift lie offset from the BPT star-forming sequence at $z = 0$ as illustrated by the small sample of $z \sim 2$ galaxies in Fig. 3.

In Cullen et al. (2013) we show that the galaxies in our sample are consistent with the elevated ionization parameters at $z \sim 2$ reported elsewhere in the literature (e.g. Nakajima et al.

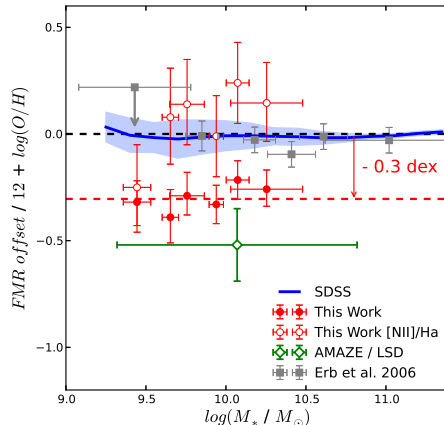


Fig. 2. Difference between the measured metallicities and the FMR prediction for various datasets. The red circles are the galaxies in our sample which are offset by ~ -0.3 dex across the full range in stellar mass. The blue line represents the original SDSS sample from Mannucci et al. (2010) with the shaded region representing the $\pm 1 \sigma$ dispersion. The grey squares are the data from Erb et al. (2006) and the green diamond a combination of $z \sim 3 - 4$ galaxies from the AMAZE/LSD surveys (Maiolino et al. 2008; Mannucci et al. 2009). The open red circles show the metallicities for our sample re-derived from the $[\text{NII}]/\text{H}\alpha$ ratios calculated using the $z \sim 2$ star-forming sequence on the BPT diagram from Kewley et al. (2013).

2013), and also our measured $[\text{OIII}]\lambda 5007/\text{H}\beta$ ratios are consistent with current $z \sim 2$ galaxies on the BPT (see Fig. 3). We conclude our galaxy sample is consistent with being offset from the $z = 0$ star-forming sequence in the BPT diagram.

In a recent theoretical work, Kewley et al. (2013) investigate how the evolution of physical conditions in star-forming regions can explain this offset in the BPT diagram in terms of the ionization parameter and elevated electron densities of high redshift galaxies. They provide a redshift dependent formulation of the BPT star-forming sequence which is illustrated in Fig. 3. Working backwards from the Kewley et al. (2013) star-forming sequence at $z \sim 2$

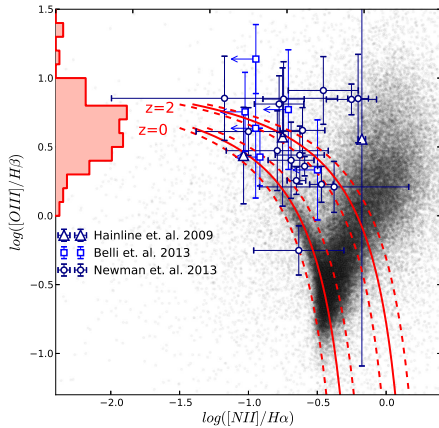


Fig. 3. BPT diagram showing the evolution of the star-forming sequence of galaxies between $z = 0$ and $z \sim 2$. In grey are a sample of SDSS galaxies, and in blue a small selection of $z \sim 2$ galaxies from the literature (Hainline et al. 2009; Belli et al. 2013; Newman et al. 2013). The red histogram on the y-axis shows the distribution of $[\text{OIII}]\lambda 5007/\text{H}\beta$ ratios for the individual galaxies in our sample. The solid red lines represent the star-forming sequence on the BPT diagram at $z = 0$ and $z \sim 2$ taken from the theoretical model of Kewley et al. (2013).

we can convert the measured $[\text{OIII}]\lambda 5007/\text{H}\beta$ ratios of our galaxy stacks in to a theoretical $[\text{NII}]/\text{H}\alpha$ ratio and recalculate the metallicity from the Maiolino et al. (2008) calibrations. The resulting metallicities are shifted by $\sim +0.3$ dex into better agreement with the FMR predictions (see Fig. 2). This result implies that the local empirical metallicity calibrations of Maiolino et al. (2008) do not fully account for the change in ionization conditions at high redshift assuming the Kewley et al. (2013) models, and in this case the discrepancy we observe with the Erb et al. (2006) data, and the FMR, may be an effect of using locally calibrated metallicity diagnostics.

5. Summary

We observe a MZR at $z \geq 2$ consistent with the shape of the MZR at $z = 0 - 3$, but which is

offset from the previous $z \geq 2$ MZR of Erb et al. (2006) to lower metallicities. The offset cannot be reconciled using the FMR and we observe an offset from the FMR at $z \geq 2$ comparable to the offset previously observed at $z \sim 3 - 4$.

This offset can be explained using the evolution of galaxies in the BPT diagram. From the data currently available it seems that the physical conditions of star-forming galaxies at $z \geq 2$ evolve in a way which is not purely metallicity dependent but depends also on a change in ionization parameter and electron density. In this scenario our results imply that metallicity calibrations derived from local galaxies will become inconsistent at high redshift. Specifically the offset in the BPT diagram suggests that metallicities derived from oxygen lines and $\text{H}\beta$ will diverge from those derived from the $[\text{NII}]/\text{H}\alpha$ ratio.

If this is the case the currently reported evolution of the FMR at high redshifts may be an artifact of the metallicity calibration and line diagnostics used.

References

- Baldwin, J. A., Phillips, M. M., & Terlevich, R. 1981, *PASP*, 93, 5
- Belli, S., et al. 2013, *ApJ*, 772, 141
- Brammer, G. B., et al. 2012, *ApJS*, 200, 13
- Cullen, F., et al. 2013, *ArXiv Astrophysics e-prints*, 1310, *MNRAS*, in press
- Daddi, E., et al. 2007, *ApJ*, 670, 156
- Erb, D. K., et al. 2006, *ApJ*, 644, 813
- Grogin, N. A., et al. 2011, *ApJS*, 197, 35
- Hainline, K. N., et al. 2009, *ApJ*, 701, 52
- Juneau, N. A., et al. 2011, *ApJ*, 736, 104
- Kewley, L. J., & Ellison, S., L. 2008, *ApJ*, 681, 1183
- Kewley, L. J., et al. 2013, *ApJ*, 774, 100
- Koekemoer, S., et al. 2011, *ApJS*, 197, 36
- Maiolino, R., et al. 2008, *A&A*, 488, 463
- Mannucci, F., et al. 2009, *MNRAS*, 398, 1915
- Mannucci, F., et al. 2010, *MNRAS*, 208, 2115
- Nakajima, K., et al. 2013, *ApJ*, 769, 3
- Newman, S. F., et al. 2013, *ArXiv Astrophysics e-prints*, 1306, *ApJ*, in press
- Tremonti, C. A., et al. 2004, *ApJ*, 613, 898